

1 **An intercomparison of oceanic methane and nitrous oxide measurements**

2
3 Samuel T. Wilson^{1*}, Hermann W. Bange², Damian L. Arévalo-Martínez², Jonathan Barnes³,
4 Alberto V. Borges⁴, Ian Brown⁵, John L. Bullister⁶, Macarena Burgos^{1,7}, David W. Capelle⁸,
5 Michael Casso⁹, Mercedes de la Paz^{10†}, Laura Farías¹¹, Lindsay Fenwick⁸, Sara Ferrón¹, Gerardo
6 Garcia¹¹, Michael Glockzin¹², David M. Karl¹, Annette Kock², Sarah Laperriere¹³, Cliff S.
7 Law^{14,15}, Cara C. Manning⁸, Andrew Marriner¹⁴, Jukka-Pekka Myllykangas¹⁶, John W.
8 Pohlman⁹, Andrew P. Rees⁵, Alyson E. Santoro¹³, Philippe D. Tortell⁸, Robert C. Upstill-
9 Goddard³, David P. Wisegarver⁶, Guiling L. Zhang¹⁷, Gregor Rehder¹²

10

11 ¹University of Hawai'i at Manoa, Daniel K. Inouye Center for Microbial Oceanography:
12 Research and Education (C-MORE), Honolulu, Hawai'i, USA

13 ²GEOMAR Helmholtz Centre for Ocean Research Kiel, Düsternbrooker Weg 20 24105 Kiel,
14 Germany

15 ³Newcastle University, School of Natural and Environmental Sciences, Newcastle upon Tyne,
16 UK

17 ⁴Université de Liège, Unité d'Océanographie Chimique, Liège, Belgium

18 ⁵Plymouth Marine Laboratory, Plymouth, UK

19 ⁶National Oceanic and Atmospheric Administration, Pacific Marine Environmental Laboratory,
20 Seattle, Washington, USA

21 ⁷Universidad de Cádiz, Instituto de Investigaciones Marinas, Departamento Química-Física
22 Cádiz, Spain

23 ⁸University of British Columbia, Vancouver, Department of Earth, Ocean and Atmospheric
24 Sciences, British Columbia, Canada

25 ⁹U.S. Geological Survey, Woods Hole Coastal and Marine Science Center, Woods Hole, USA

26 ¹⁰Instituto de Investigaciones Marinas, Vigo, Spain

27 ¹¹University of Concepción, Department of Oceanography and Center for climate research and
28 resilience (CR2), Concepción, Chile

29 ¹²Leibniz Institute for Baltic Sea Research Warnemünde, Rostock, Germany

30 ¹³University of California Santa Barbara, Department of Ecology, Evolution, and Marine
31 Biology, Santa Barbara, USA

32 ¹⁴National Institute of Water and Atmospheric Research (NIWA), Wellington, New Zealand

33 ¹⁵Department of Chemistry, University of Otago, Dunedin, New Zealand

34 ¹⁶University of Helsinki, Department of Environmental Sciences, Helsinki, Finland

35 ¹⁷Ocean University of China, Department of Marine Chemistry, Qingdao, China

36

37 †Current address: Instituto Español de Oceanografía, Centro Oceanográfico de A Coruña, A

38 Coruña, Spain

39

40 *corresponding author: stwilson@Hawaii'i.edu

41 **Abstract.** Large scale climatic forcing is impacting oceanic biogeochemical cycles and is
42 expected to influence the water-column distribution of trace gases including methane and nitrous
43 oxide. Our ability as a scientific community to evaluate changes in the water-column inventories
44 of methane and nitrous oxide depends largely on our capacity to obtain robust and accurate
45 concentration measurements which can be validated across different laboratory groups. This
46 study represents the first formal, international, intercomparison of oceanic methane and nitrous
47 oxide measurements whereby participating laboratories received batches of seawater samples
48 from the subtropical Pacific Ocean and the Baltic Sea. Additionally, compressed gas standards
49 from the same calibration scale were distributed to the majority of participating laboratories to
50 improve the analytical accuracy of the gas measurements. The computations used by each
51 laboratory to derive the dissolved gas concentrations were also evaluated for inconsistencies (*e.g.*
52 pressure and temperature corrections, solubility constants). The results from the intercomparison
53 and intercalibration provided invaluable insights into methane and nitrous oxide measurements.
54 It was observed that analyses of seawater samples with the lowest concentrations of methane and
55 nitrous oxide had the lowest precisions. In comparison, while the analytical precision for
56 samples with the highest concentrations of trace gases was better, the variability between the
57 different laboratories was higher; 36% for methane and 27% for nitrous oxide. In addition, the
58 comparison of different batches of seawater samples with methane and nitrous oxide
59 concentrations that ranged over an order of magnitude revealed the ramifications of different
60 calibration procedures for each trace gas. Finally, this study builds upon the intercomparison
61 results to develop recommendations for improving oceanic methane and nitrous oxide
62 measurements, with the aim of precluding future analytical discrepancies between laboratories.

63 1. Introduction

64 The increasing mole fractions of greenhouse gases in the Earth's atmosphere are causing long-
65 term climate change with unknown future consequences. Two greenhouse gases, methane and
66 nitrous oxide, together contribute approximately 23% of total radiative forcing attributed to well-
67 mixed greenhouse gases (Myhre et al., 2013). It is imperative that the monitoring of methane
68 and nitrous oxide in the Earth's atmosphere is accompanied by measurements at the Earth's
69 surface to better inform the sources and sinks of these climatically important trace gases. This
70 includes measurements of dissolved methane and nitrous oxide in the marine environment,
71 which is an overall source of both gases to the overlying atmosphere (Nevison et al., 1995;
72 Anderson et al., 2010; Naqvi et al., 2010; Freing et al., 2012; Ciais et al., 2014).

73 Oceanic measurements of methane and nitrous oxide are conducted as part of established
74 time-series locations, along hydrographic survey lines, and during disparate oceanographic
75 expeditions. Within low to mid-latitude regions of the open ocean, the surface waters are
76 frequently slightly super-saturated with respect to atmospheric equilibrium for both methane and
77 nitrous oxide. There is typically an order of magnitude range in concentration along a vertical
78 water-column profile at any particular open ocean location (e.g. Wilson et al., 2017). In contrast
79 to the open ocean, near-shore environments, which are subject to river inputs, coastal upwelling,
80 benthic exchange and other processes, have higher concentrations and greater spatial and
81 temporal heterogeneity (e.g. Schmale et al., 2010; Upstill-Goddard and Barnes, 2016).

82 Methods for quantifying dissolved methane and nitrous oxide have evolved and somewhat
83 diverged since the first measurements were made in the 1960s (Craig and Gordon 1963;
84 Atkinson and Richards 1967). Some laboratories employ purge-and-trap methods for extracting
85 and concentrating the gases prior to their analysis (e.g. Zhang et al., 2004; Bullister and
86 Wisegarver, 2008; Capelle et al., 2015; Wilson et al., 2017). Others equilibrate a seawater
87 sample with an overlying headspace gas and inject a fixed volume of the gaseous phase into a
88 gas analyzer (e.g. Upstill-Goddard et al., 1996; Walter et al., 2005; Farias et al., 2009). The
89 purge and trap technique is typically more sensitive by 1-2 orders of magnitude over headspace
90 equilibrium (Magen et al., 2014; Wilson et al., 2017). However, the purge and trap technique
91 requires more time for sample analysis and it is more difficult to automate the injection of
92 samples into the gas analyzer. Headspace equilibrium sampling is most suited for volatile
93 compounds that can be efficiently partitioned into the headspace gas volume from the seawater

94 sample. Its limited sensitivity can be compensated by large volume analysis (*e.g.* Upstill-
95 Goddard et al., 1996). Additional developments for continuous underway surface seawater
96 measurements use equilibrators systems of various designs coupled to a variety of detectors (*e.g.*
97 Weiss et al., 1992; Butler et al., 1989; Gülzow et al., 2011; Arévalo-Martínez et al., 2013).
98 Determining the level of analytical comparability between different laboratories for discrete
99 samples of methane and nitrous oxide is an important step towards improved comprehensive
100 global assessments. Such intercomparison exercises are critical to determining the spatial and
101 temporal variability of methane and nitrous oxide across the world oceans with confidence, since
102 no single laboratory can single-handedly provide all the required measurements at sufficient
103 resolution. Previous comparative exercises have been conducted for other trace gases *e.g.* carbon
104 dioxide, dimethylsulphide, and sulfur hexafluoride (Dickson et al., 2007; Bullister and Tanhua,
105 2010; Swan et al., 2014) and for trace elements (Cutter et al., 2013). These exercises confirm the
106 value of the intercomparison concept.

107 To instigate this process for methane and nitrous oxide, a series of international
108 intercomparison exercises were conducted between 2013 and 2017, under the auspices of
109 Working Group #143 of the Scientific Committee on Oceanic Research (SCOR) ([www.scor-](http://www.scor-int.org)
110 [int.org](http://www.scor-int.org)). Discrete seawater samples collected from the subtropical Pacific Ocean and the Baltic
111 Sea were distributed to the participating laboratories (Table 1). The samples were selected to
112 cover a representative range of concentrations across marine locations, from the oligotrophic
113 open ocean to highly productive waters, and in some instances sub-oxic, coastal waters. An
114 integral component of the intercomparison exercise was the production and distribution of
115 methane and nitrous oxide gas standards to members of the SCOR Working Group. The
116 intercomparison exercise was conceived and evaluated with the following four questions in
117 mind:

118 Q1. What is the agreement between the SCOR gas standards and the ‘in-house’ gas standards
119 used by each laboratory?

120 Q2. How do measured values of dissolved methane and nitrous oxide compare across
121 laboratories?

122 Q3. Despite the use of different analytical systems, are there general recommendations to reduce
123 uncertainty in the accuracy and precision of methane and nitrous oxide measurements?

124 Q4. What are the implications of inter-laboratory differences for determining the spatial and
125 temporal variability of methane and nitrous oxide in the oceans?
126

127 **2. Methods**

128 **2.1 Calibration of nitrous oxide and methane using compressed gas standards**

129 Laboratory-based measurements of oceanic methane and nitrous oxide require separation of the
130 dissolved gas from the aqueous phase, with the analysis conducted on the gaseous phase.
131 Calibration of the analytical instrumentation used to quantify the concentration of methane and
132 nitrous oxide is nearly always conducted using compressed gas standards, the specifics of which
133 vary between each laboratory. Therefore, the reporting of methane and nitrous oxide datasets
134 ought to be accompanied by a description of the standards used, including their methane and
135 nitrous oxide mole fractions, the declared accuracies, and the composition of their balance or
136 ‘make-up’ gas. For both gases, the highest accuracy commercially available standards have
137 mole fractions close to current day atmospheric values. These standards can be obtained from
138 national agencies including National Oceanic and Atmospheric Administration Global
139 Monitoring Division (NOAA GMD), the National Institute of Metrology China, and the Central
140 Analytical Laboratories of the European Integrated Carbon Observation System Research
141 Infrastructure (ICOS-RI). By comparison, it is more difficult to obtain highly accurate methane
142 and nitrous oxide gas standards with mole fractions exceeding modern-day atmospheric values.
143 This is particularly problematic for nitrous oxide due to the nonlinearity of the widely used
144 Electron Capture Detector (ECD) (Butler and Elkins, 1991).

145 The absence of a widely available high mole fraction, high accuracy nitrous oxide gas
146 standard was noted as a primary concern at the outset of the intercomparison exercise.
147 Therefore, a set of high-pressure primary gas standards was prepared for the SCOR Working
148 Group by John Bullister and David Wisegarver at NOAA Pacific Marine and Environmental
149 Laboratory (PMEL). One batch, referred to as Air Ratio Standard (ARS), had methane and
150 nitrous oxide mole fractions similar to modern air and the other batch, referred to as Water Ratio
151 Standard (WRS) had higher methane and nitrous oxide mole fractions for calibration of high
152 concentration water samples. These SCOR primary standards were checked for stability over a
153 12 month period and assigned mole fractions on the same calibration scale, known as ‘SCOR-
154 2016.’ A comparison was conducted with NOAA standards prepared on the SIO98 calibration

155 scale for nitrous oxide and the NOAA04 calibration scale for methane. Based on the comparison
156 with NOAA standards, the uncertainty of the methane and nitrous oxide mole fractions in the
157 ARS and the uncertainty of the methane mole fraction in the WRS were all estimated at better
158 than 1%. By contrast, the uncertainty of the nitrous oxide mole fraction in the WRS was
159 estimated at 2-3%. The gas standards were distributed to twelve of the laboratories involved in
160 this study (Table 1). The technical details on the production of the gas standards and their
161 assigned absolute mole fractions is included in Bullister et al. (2016).

162

163 **2.2 Collection of discrete samples of nitrous oxide and methane**

164 Dissolved methane and nitrous oxide samples for the intercomparison exercise were collected
165 from the subtropical Pacific Ocean and the Baltic Sea. Pacific samples were obtained on 28
166 November 2013 and 24 February 2017 from the Hawai'i Ocean Time-series (HOT) long-term
167 monitoring site, Station ALOHA, located at 22.75 N, 158.00 W. The November 2013 samples
168 are included in Figure S1 and S2 in the Supplement, but are not discussed in the main Results or
169 Discussion because fewer laboratories were involved in the initial intercomparison, and the
170 results from these samples support the same conclusions obtained with the more recent sample
171 collections. Seawater was collected using Niskin-like bottles designed by John Bullister (NOAA
172 PMEL), which help minimize contamination of trace gases, in particular chlorofluorocarbons
173 and sulfur hexafluoride (Bullister and Wisegarver, 2008). The bottles were attached to a rosette
174 with a conductivity-temperature-depth (CTD) package. Seawater was collected from two depths:
175 700 m and 25 m, where the near-maximum and minimum water-column concentrations for
176 methane and nitrous oxide at this location can be found. **The 25 m samples were always well
177 within the surface mixed layer, which ranged from 100 to 130 m depth during sampling.**

178 Replicate samples were collected from each bottle, with one replicate reserved for analysis at the
179 University of Hawai'i to evaluate variability between sampling bottles. Seawater was dispensed
180 from the Niskin-like bottles using Tygon® tubing into the bottom of borosilicate glass bottles,
181 allowing overflow of at least two sample volumes and ensuring the absence of bubbles. Most
182 sample bottles were 240 mL in size and were sealed with no headspace using butyl-rubber
183 stoppers and aluminum crimp-seals. A few laboratory groups requested smaller crimp-sealed
184 glass bottles ranging from 20-120 mL in volume and two laboratories used 1 L glass bottles
185 which were closed with a glass stopper and sealed with Apiezon® grease. Seawater samples

186 were collected in quadruplicate for each laboratory. All samples were preserved using saturated
187 mercuric chloride solution (100 μL of saturated mercuric chloride solution per 100 mL of
188 seawater sample) and stored in the dark at room temperature until shipment. **The choice of**
189 **mercuric chloride as the preservative for dissolved methane and nitrous oxide was due to its long**
190 **history of usage. It is recognized that other preservatives have been proposed (e.g. Magen et al.,**
191 **2014, Bussmann et al., 2015), however pending a community-wide evaluation of their**
192 **effectiveness over a range of microbial assemblages and environmental conditions for both**
193 **methane and nitrous oxide, it is not evident that they are a superior alternative to mercuric**
194 **chloride.**

195 Samples from the western Baltic Sea were collected during 15-21 October 2016, onboard the
196 R/V *Elisabeth Mann Borgese* (Table 2). Since the Baltic Sea consists of different basins with
197 varying concentrations of oxygen beneath permanent haloclines (Schmale et al., 2010), a larger
198 range of water-column methane and nitrous oxide concentrations were accessible for inter-
199 laboratory comparison compared to Station ALOHA. For all seven Baltic Sea stations, the
200 water-column was sampled into an on-deck 1,000 L water tank that was subsequently
201 subsampled into discrete sample bottles. At three stations (BAL1, BAL3, and BAL6), the water
202 tank was filled from the shipboard high-throughput underway seawater system. For deeper
203 water-column sampling at the stations BAL2, BAL4, and BAL5, the water tank was filled using
204 a pumping CTD system (Strady et al., 2008) with a flow rate of 6 L min^{-1} and a total pumping
205 time of approximately 3 h. For the final deep water-column station, BAL7, the pump that
206 supplied the shipboard underway system was lowered to a depth of 21 m to facilitate a shorter
207 pumping time of approximately 20 mins. Subsampling the water tank for all samples took
208 approximately 1 h in total and the total sampling volume was less than 100 L. To verify the
209 homogeneity of the seawater during the sampling process, the first and last samples collected
210 from the water tank were analyzed by Newcastle University onboard the research vessel. In
211 contrast to the Pacific Ocean sampling, which predominantly used 240 mL glass vials, each
212 laboratory provided their own preferred vials and stoppers for the Baltic Sea samples. Seawater
213 samples were collected in triplicate for each laboratory. All samples were preserved with 100
214 μL of saturated mercuric chloride solution per 100 ml of seawater sample, with the exception of
215 samples collected by U.S. Geological Survey, who analyzed unpreserved samples onboard the
216 research vessel.

217

218 **2.3. Sample analysis**

219 Each laboratory measured dissolved methane and nitrous oxide slightly differently. A full
220 description of each laboratory's method can be found in Table S6 and Table S7 in the
221 Supplement for methane and nitrous oxide, respectively.

222 The majority of laboratories measured methane and nitrous oxide by equilibrating the
223 seawater sample with an overlying headspace and subsequently injecting a portion of the gaseous
224 phase into the gas analyzer. This method has been conducted since the 1960s when gas
225 chromatography was first used to quantify dissolved hydrocarbons (McAuliffe, 1963). The
226 headspace was created using helium, nitrogen, or high-purity air to displace a portion of the
227 seawater sample within the sample bottle. Alternatively, a subsample of the seawater was
228 transferred to a gas-tight syringe and the headspace gas subsequently added. The volume of the
229 vessel used to conduct the headspace equilibration ranged from 20 ml borosilicate glass vials to 1
230 L glass vials and syringes used by Newcastle University and U.S. Geological Survey,
231 respectively. The dissolved gases equilibrated with the overlying headspace at a controlled
232 temperature for a set period of time that ranged from 20 min to 24 h for the different laboratories.
233 The longer equilibration times are due to overnight equilibrations in water baths. The majority
234 of laboratories enhanced the equilibration process by some initial period of physical agitation.
235 After equilibration, an aliquot of the headspace was transferred into the gas analyzer (GA) by
236 either physical injection, displacement using a brine solution, or injection using a switching
237 valve. Some laboratories incorporated a drying agent and a carbon dioxide scrubber prior to
238 analysis. The gas sample passed through a multi-port injection valve containing a sample loop of
239 known volume, which transferred the gas sample directly onto the analytical column within the
240 oven of the GA. Calibration of the instrument was achieved by passing the gas standards
241 through the injection valve.

242 The final gas concentrations using the headspace equilibration method was calculated by:

243

$$244 \quad [1] \quad C_{gas} [\text{nmol L}^{-1}] = \left(\beta x P V_{wp} + \frac{xP}{RT} V_{hs} \right) / V_{wp}$$

245

246 where β is the Bunsen solubility of nitrous oxide (Weiss and Price, 1980) or methane
247 (Wiesenburg and Guinasso, 1979) in $\text{nmol L}^{-1} \text{atm}^{-1}$, x is the dry gas mole fraction (ppb)

248 measured in the headspace, P is the atmospheric pressure (atm), V_{wp} is the volume of water
249 sample (mL), V_{hs} is the volume (mL) of the created headspace, R is the gas constant (0.08205746
250 L atm K⁻¹mol⁻¹), and T is equilibration temperature in Kelvin (K). An example calculation is
251 provided in Table S8 in the Supplement.

252 In contrast to the headspace equilibrium method, five laboratories used a purge-and-trap
253 system for methane and/or nitrous oxide analysis (Table S6 and Table S7 in the Supplement).
254 These systems were directly coupled to a Flame Ionization Detector (FID) or ECD, with the
255 exception of University of British Columbia, where a quadrupole mass spectrometer with an
256 electron impact ion source and Faraday cup detector were used (Capelle et al., 2015). The
257 purge-and-trap systems were broadly similar, each transferring the seawater sample to a sparging
258 chamber. Sparging times typically ranged from 5-10 min and the sparge gas was either high
259 purity helium or high purity nitrogen. **In addition to commercially available gas scrubbers,**
260 **purification of the sparge gas was achieved by passing it through stainless steel tubing packed**
261 **with Poropak Q and immersed in liquid nitrogen. This is a recommended precaution to**
262 **consistently achieve a low blank signal of methane.** The elutant gas was dried using Nafion or
263 Drierite, and subsequently cryotrapped on a sample loop packed with Porapak Q to aid retention
264 of methane and nitrous oxide. **Cryotrapping was achieved for methane using liquid nitrogen (-**
265 **195°C) and either liquid nitrogen or cooled ethanol (-70°C) for nitrous oxide.** Subsequently, the
266 valve was switched to inject mode and the sample loop was rapidly heated to transfer its contents
267 onto the analytical column. Calibration was achieved by injecting standards via sample loops
268 using multi-port injection valves. Injection of standards upstream of the sparge chamber allowed
269 for calibration of the purge-and-trap gas handling system, in addition to the GA. Calculation of
270 the gas concentrations using the purge-and-trap method was achieved by application of the ideal
271 gas law to the standard gas measurements:

$$272 \quad [2] \quad PV = nRT$$

273 where P , R , and T are the same as Equation 1, V represents the volume of gas injected (L),
274 and n represents moles of gas injected. Rearranging Equation 2 yields the number of moles of
275 methane or nitrous oxide gas for each sample loop injection of compressed gas standards. These
276 values were used to determine a calibration curve based on the measured peak areas of the
277 injected standards, and thereafter derive the number of moles measured for each unknown
278 sample. To calculate concentrations of methane or nitrous oxide in a water sample, the number

279 of moles measured were divided by the volume (L) of seawater sample analyzed. An example
280 calculation is provided in Table S8 in the Supplement.

281

282 **2.4 Data analysis**

283 The final concentrations of methane and nitrous oxide are reported in nmol kg^{-1} . The analytical
284 precision for each batch of samples obtained by each of the individual laboratories was estimated
285 from the analysis of replicate seawater samples and reported as the coefficient of variation (%).

286 The values reported by each laboratory for all the batches of seawater samples are shown in
287 Tables S1 to S4 in the Supplement. Due to the observed inter-laboratory variability, it is likely
288 that the median value of methane and nitrous oxide for each batch of samples does not represent
289 the absolute *in situ* concentration. As this complicates the analytical accuracy for each
290 laboratory, we instead calculated the percentage difference between the median concentration
291 determined for each set of samples and the mean value reported by an individual laboratory. The
292 presence of outliers was established using the Interquartile Range (IQR) and by comparing with
293 one standard deviation applied to the overall median value.

294

295 **3. Results**

296 **3.1 Comparison of methane and nitrous oxide gas standards**

297 Six laboratories compared their existing ‘in-house’ standards of methane with the SCOR
298 standards. This was done by calibrating in-house standards and deriving a mixing ratio for the
299 SCOR standards which were treated as unknowns. Four laboratories reported methane values for
300 either the ARS or WRS within 3% of their absolute concentration, whereas two laboratories
301 reported an offset of 6% and 10% between their in-house standards and the SCOR standards
302 (Table S6 in the Supplement). For those laboratories who measured the SCOR standards to
303 within 3% or better accuracy, observed offsets in methane concentrations from the overall
304 median cannot be due to the calibration gas.

305 Seven laboratories compared their own in-house standards of nitrous oxide with the prepared
306 SCOR standards. Six laboratories reported values of nitrous oxide for the ARS which were
307 within 3% of the absolute concentration, with the remaining laboratory reporting an offset of
308 10% (Table S7 in the Supplement). The majority of these laboratories (five out of six groups)
309 compared the SCOR ARS with NOAA GMD standards, which have a balance gas of air instead

310 of nitrogen. Some laboratories with analytical systems that incorporated fixed sample loops (*e.g.*
311 1 or 2 ml loops housed in a 6-port or 10-port injection valve) had difficulty analyzing the WRS,
312 as the peak areas created by the high mole fraction of the standard exceeded the signal typically
313 measured from in-house standards or acquired by sample analysis, by an order of magnitude.
314 The high mole fraction of the WRS was not an issue when multiple sample loops of varying
315 sizes were incorporated into the analytical system, which was the case for purge-and-trap based
316 designs. For the two laboratories with an in-house standard of comparable mole fraction to the
317 WRS, an offset of 3% and a >20% offset was reported.

318

319 **3.2 Methane concentrations in the intercomparison samples**

320 Overall, median methane concentrations in seawater samples collected from the Pacific Ocean
321 and the Baltic Sea ranged from 0.9 to 60.3 nmol kg⁻¹ (Table 2). Out of 101 reported values, 3
322 outliers were identified using the IQR criterion and were not included in further analysis. The
323 methane data values for each batch of samples analyzed by each laboratory, including the mean
324 and standard deviation, the number of samples analyzed, and the % offset from the overall
325 median value are reported in Table S1 and Table S2 in the Supplement. Analysis conducted by
326 the University of Hawai'i of methane and nitrous oxide from each Niskin-like bottle used in the
327 Pacific Ocean sampling did not reveal any bottle-to-bottle differences. Furthermore, analysis by
328 Newcastle University showed there was no difference between the first and the last set of
329 samples collected from the 1000 L collection used in the Baltic Sea sampling.

330 The two Pacific Ocean sampling sites had the lowest water-column concentrations of
331 methane (Fig. 1a and 1b). The PAC1 samples collected from within the mesopelagic zone,
332 where methane concentrations have been reported to be less than 1 nmol kg⁻¹ (Reeburgh, 2007;
333 Wilson et al., 2017), showed a distribution of reported concentrations skewed towards the higher
334 values. For the PAC1 samples, seven out of twelve laboratories reported values ≤ 1 nmol kg⁻¹
335 and the mean coefficient of variation for all laboratories was 11% (Table 2). In contrast to the
336 mesopelagic samples, the methane concentrations for the near-surface seawater samples (PAC2)
337 were close to atmospheric equilibrium (Fig. 1b). Measured concentrations of methane for PAC2
338 samples ranged from 1.9 to 3.8 nmol kg⁻¹ and the mean coefficient of variation for all
339 laboratories was 7%. Similar to the PAC1 samples, PAC2 also had a distribution of data skewed
340 towards the higher concentrations.

341 Three Baltic Sea sampling sites (BAL1, BAL3, and BAL6) had median methane
342 concentrations that ranged from 4.1 to 5.7 nmol kg⁻¹ (Fig. 1c). The BAL1 samples also showed a
343 skewed distribution of reported values towards higher concentrations, as seen in PAC1 and
344 PAC2 samples. However, this was not evident in BAL3 or BAL6, which had the closest
345 agreement between the reported methane concentrations. For these three sets of Baltic Sea
346 samples, the mean coefficient of variation for all laboratories ranged from 4% (BAL3) to 9%
347 (BAL1). The next three Baltic Sea samples (BAL4, BAL5, and BAL7) had methane
348 concentrations that ranged from 18.8 to 35.4 nmol kg⁻¹ (Fig. 1d). These three sets of samples
349 had a normal distribution of data and the closest agreement between the reported concentrations
350 for all of the Pacific Ocean and Baltic Sea samples. Furthermore, for these three sets of samples,
351 the mean coefficient of variation for all laboratories was 4% (Table 2). The final Baltic Sea
352 sample (BAL2) had the highest concentrations of methane, with a median reported value of 60.3
353 nmol kg⁻¹, and a large range of values (45.2 to 67.2 nmol kg⁻¹; Fig. 1e). The BAL2 samples had
354 the lowest overall mean coefficient of variation for all laboratories; 2% (Table 2).

355 Further analysis of the data was conducted to better comprehend the factors that caused the
356 observed inter-laboratory variability in methane measurements. The deviation from median
357 values was calculated for each sample collected from the Baltic Sea (Fig. 2). The Pacific Ocean
358 samples (PAC1 and PAC2) were not included in this analysis due to the skewed distribution of
359 data. There were also some instances in the Baltic Sea samples, where the median concentration
360 might not have realistically represented the absolute *in situ* methane concentration. This was
361 most likely to have occurred at low concentrations due to the skewed distribution of reported
362 concentrations (*e.g.* BAL1) or at high concentrations where there was a large range in reported
363 values (*e.g.* BAL2). The results revealed that a few laboratories (Datasets D, F, and G) were
364 consistently within or close to 5% of the median value for all batches of seawater samples (Fig.
365 2). Some laboratories (*e.g.* Datasets B, C, and H) had a higher deviation from the median value
366 at higher methane concentrations. Two laboratories (Datasets J and K) had a higher deviation
367 from the median value at lower methane concentrations. Finally, in some cases it was not
368 possible to determine a trend (Datasets A and E), due to the variability.

369 The reasons behind the trends for each dataset became more apparent when considering the
370 effect of the inclusion or exclusion of low standards in the calibration curve on the resulting
371 derived concentrations (Fig. 3). The FID has a linear response to methane at nanomolar values

372 and therefore a high level of accuracy across a relatively wide range of *in situ* methane
373 concentrations can be obtained with the correct slope and intercept. To demonstrate this,
374 calibration curves for methane were provided by the University of Hawai'i. These revealed
375 minimal variation in the slope value when calibration points were increased from low mole
376 fractions (Fig. 3a) to higher mole fractions (Fig. 3b). However, the intercept value was sensitive
377 to the range of calibration values used, and this effect was further exacerbated when only the
378 higher calibration points were included (*i.e.* Fig. 3c). **The relevance to final methane**
379 **concentrations is demonstrated by considering the values reported by the University of Hawai'i**
380 **for PAC2 samples (Fig. 1b). An almost 30% increase in final methane concentration occurs**
381 **from the use of the calibration equation in Figure 3c, compared to Figure 3a. This derives from a**
382 **measured peak area for methane of 62 for a sample with a volume of 0.076 L and a seawater**
383 **density of 1024 kg m⁻³, yielding a final methane concentration of 2.1 and 2.8 nmol kg⁻¹ using the**
384 **equations from Figure 3a and 3c, respectively. With this understanding on the effect of FID**
385 **calibration, we consider it likely that the increased deviation from median values at high methane**
386 **concentrations (Datasets B, C, and H) results from differences in calibration slope between each**
387 **laboratory. In contrast, the datasets with a higher offset at low methane concentrations (Datasets**
388 **J and K) could be due to erroneous low standard values causing a skewed intercept. In addition,**
389 **there may be other factors including sample contamination, discussed in Section 3.4.**

390

391 **3.3 Nitrous oxide concentrations in the intercomparison samples**

392 Overall, median nitrous oxide concentrations in seawater samples collected from the Pacific
393 Ocean and the Baltic Sea ranged from 3.4 to 42.4 nmol kg⁻¹ (Table 2). Of the 113 reported
394 values, ten outliers were identified using the IQR criterion and were not included in further
395 analysis. The nitrous oxide data values for each batch of samples analyzed by each laboratory,
396 including the mean and standard deviation, the number of samples analyzed, and the % offset
397 from the overall median value are reported in Table S3 and Table S4 in the Supplement.

398 For six sets of seawater samples, BAL1, BAL2, BAL3, BAL6, BAL7, and PAC2, the
399 concentrations of nitrous oxide were close to atmospheric equilibrium. The reported values
400 ranged from 7.7 to 12.7 nmol kg⁻¹ in the Baltic Sea (Fig. 4a) and from 5.9 to 7.6 nmol kg⁻¹ in the
401 Pacific Ocean (Fig. 4b). For the Pacific Ocean near-surface (**mixed layer**) sampling site (PAC2),
402 the theoretical value of nitrous oxide concentration in equilibrium with the overlying atmosphere

403 is also shown (Fig. 4b). For these six samples with concentrations close to atmospheric
404 equilibrium, the mean coefficient of variation for all laboratories ranged from 3% (BAL3 and
405 PAC2) to 5% (BAL1) (Table 2).

406 For the three other sets of samples (BAL4, BAL5, and PAC1), the nitrous oxide
407 concentrations deviated significantly from atmospheric equilibrium (Fig. 4c, 4d, and 4e). At one
408 sampling site, BAL4 (Fig. 4c), nitrous oxide was under-saturated with respect to atmospheric
409 equilibrium and reported concentrations ranged from 2.1–5.5 nmol kg⁻¹. As observed in the low
410 concentration Pacific Ocean methane samples, there was a skewed distribution of the data
411 towards the higher nitrous oxide concentrations. The BAL4 samples also had the highest
412 variability (*i.e.* lowest precision), with a mean coefficient of variation of 8% (Table 2). The two
413 remaining samples (PAC1 and BAL5) had much higher concentrations of nitrous oxide, as
414 expected for low-oxygen regions of the water-column. In contrast to the samples with near
415 atmospheric equilibrium concentrations of nitrous oxide, there was a low overall agreement
416 between the independent laboratories for PAC1 and BAL5 nitrous oxide concentrations (Fig. 4d,
417 4e). At PAC1 and BAL5, nitrous oxide concentrations ranged from 34.3–45.8 nmol kg⁻¹ (Fig.
418 4d) and 30.1–45.9 nmol kg⁻¹, respectively (Fig. 4e). The mean coefficient of variation for all
419 laboratories was 4% for BAL5 samples compared to 3% for PAC1 samples.

420 The deviation of individual nitrous oxide concentrations from the median value provides
421 insight into the variability associated with their measurements (Fig. 5). The BAL1 dataset was
422 not included in this analysis due to its skewed data distribution and the high inter-laboratory
423 variability for BAL5 indicated that the median value may differ from the absolute nitrous oxide
424 concentration for this sample. For the low nitrous oxide Baltic Sea and Pacific Ocean samples
425 (Fig. 5a), the majority of data points were within 5% of the median values. Furthermore, for the
426 majority of laboratories, the data points for separate seawater samples clustered together
427 indicating some consistency to the extent they varied from the overall median value. Exceptions
428 to this observation include Datasets E, C, L, and K (Fig. 5a) which demonstrated varying
429 precision and accuracy. At high nitrous oxide concentrations (Fig. 5b), there are fewer data
430 points within 5% of the median value compared to low nitrous oxide concentrations (Fig. 5a).
431 Therefore, for PAC1 and BAL5 samples, 6 and 7 data points fall within 5% of the median value,
432 respectively. Furthermore, only three laboratories (Datasets F, G, and K) had data for both
433 Pacific Ocean and Baltic Sea samples within 5% of the median value. This could have been

434 caused by inconsistent analysis between different batches of samples or by variable sample
435 collection and transportation.

436 The likely factors that caused these offsets in nitrous oxide concentrations among
437 laboratories include sample analysis and calibration of the gas analyzers. Calibration of the ECD
438 is nontrivial and at least two prior publications have discussed nitrous oxide calibration issues
439 (Butler and Elkins, 1991; Bange et al., 2001). The laboratories participating in the nitrous oxide
440 intercomparison employed different calibration procedures (Fig. 6). Some used a linear fit and
441 kept their analytical peak areas within a narrow range (Fig. 6a), while others used a step-wise
442 linear fit and therefore used different slopes for low and high nitrous oxide mole fractions (Fig.
443 6b). Finally, some applied a polynomial curve (Fig. 6c) and sometimes two different polynomial
444 fits, for low and high concentrations. The difficulty in calibrating the ECD was evidenced by the
445 deviation from median values as multiple datasets show good precision but consistent offsets at
446 the lowest (Fig. 5a) and highest (Fig. 5b) final concentrations of nitrous oxide.

447

448 **3.4 Sample storage and sample bottle size**

449 Because prolonged storage of samples can influence dissolved gas concentrations, including
450 methane and nitrous oxide, the intercomparison dataset was analyzed for sample storage effects
451 (Table S5 in the Supplement). It should, however, be noted that assessing the effect of storage
452 time on sample integrity was not a formal goal of the intercomparison exercise and replicate
453 samples were not analyzed at repeated intervals by independent laboratories, as would normally
454 be required for a thorough analysis. Nonetheless our results did provide some insights into
455 potential storage-related problems. Most notably, there were indications that an increase in
456 storage time caused increased concentrations and increased variability for methane samples with
457 low concentrations, *i.e.* PAC1 and PAC2 samples which had median methane concentrations of
458 0.9 and 2.3 nmol kg⁻¹, respectively (Fig. 7). In comparison, for samples of nitrous oxide with
459 low concentrations there was no trend of increasing values as observed for samples with low
460 methane concentrations.

461 Another variable which differed between laboratories for the intercomparison exercise was
462 the size of samples bottle, which ranged from 25 ml to 1 liter for the different laboratories.
463 There was no observed difference between the methane and nitrous oxide values obtained from
464 the various sampling bottles and it was concluded that sampling bottles were not a controlling

465 factor for the observed differences between laboratories. We note, however, the potential for
466 greater air bubble contamination in smaller bottles.

467

468 **4. Discussion**

469 The marine methane and nitrous oxide analytical community is growing. This is reflected in the
470 increasing number of corresponding scientific publications and the resulting development of a
471 global database for methane and nitrous oxide (Bange et al., 2009). Like all Earth observation
472 measurements, there is a need for intercomparison exercises of the type reported here, for data
473 quality assurance, and for appropriate reporting practices (National Research Council, 1993). To
474 the best of our knowledge, the work presented here is the first formal intercomparison of
475 dissolved methane and nitrous oxide measurements. Based on our results, we discuss the lessons
476 learned and our recommendations moving forward, by addressing the four questions that were
477 posed in the Introduction.

478

479 **4.1 What is the agreement between the SCOR gas standards and the ‘in-house’ gas 480 standards used by each laboratory?**

481 It is typical for laboratories to source some, or all, of their compressed gas standards from
482 commercial suppliers. National agencies, such as NOAA GMD or National Institute of
483 Metrology China, also provide standards to the scientific community. The national agencies
484 typically offer a lower range in concentrations than commercial suppliers, but their standards
485 tend to have a higher level of accuracy. Of the twelve laboratories participating in the
486 intercomparison, eight reported using national agency standards, with seven of them using gases
487 sourced from NOAA GMD. Since the methane and nitrous oxide mole fractions of these
488 national agency standards are equivalent to modern-day atmospheric mixing ratios, they are
489 similar to the SCOR ARS distributed to the majority of laboratories in this study. Laboratories
490 in receipt of the SCOR standards were asked to predict their mole fractions based on those of
491 their own in-house standards. For the majority that conducted this exercise, there was good
492 agreement (<3% difference) between the NOAA GMD and the SCOR ARS for both methane
493 and nitrous oxide. For three laboratories, a larger offset was observed between the NOAA GMD
494 and the SCOR ARS. There was also a good prediction for the higher methane content SCOR
495 WRS, facilitated by the linear response of the FID (Fig. 3). In contrast, the nitrous oxide mole

496 fraction in the SCOR WRS exceeded the typical working range for several laboratories and it
497 was difficult for them to cross-compare with their in-house standards. This reflects an analytical
498 set-up that involves on-column injection via a 6-port or 10-port valve with one or two sample
499 loops, respectively. The sample loops have a fixed volume and their inaccessibility makes it
500 difficult to replace them by a smaller loop size. Therefore either dilution of the standard is
501 required, or smaller loops need to be incorporated into the calibration protocol. The two
502 laboratories that compared their in-house standards with the SCOR WRS reported an offset of
503 3% and >20%. This indicates that variability between standards can be an issue for obtaining
504 accurate dissolved concentrations and provides support for the production of a widely available
505 high concentration nitrous oxide standard. We strongly recommend that all commercially
506 obtained standards are cross-checked against primary standards, such as the SCOR ARS and
507 WRS. This should be conducted at least at the beginning and end of their use to detect any drift
508 that may have occurred during their lifetime. With due diligence and care, the SCOR standards
509 provide the capability for cross-checking personal standards for years to decades (Bullister et al.,
510 2016).

511

512 **4.2 How do measured values of methane and nitrous oxide compare across laboratories?**

513 **Methane:** The methane intercomparison highlighted the variability that exists between
514 measurements conducted by independent laboratories. At low methane concentrations, a skewed
515 distribution of methane data was observed, which was particularly evident in PAC1 (Fig. 1a).
516 Potential causes include calibration procedures (Section 3.2) and/or sample contamination which
517 is more prevalent at low concentrations (Section 3.4). For some laboratories, the low methane
518 concentrations are close to their detection limit, which is determined by the relatively low
519 sensitivity of the FID and the small number of moles of methane in an introduced headspace
520 **equilibrated** with seawater. An approximate working detection limit for methane analysis via
521 headspace equilibration is 1 nmol kg^{-1} , although some laboratories improve upon this by having
522 a large aqueous: gaseous phase ratio during the equilibration process (*e.g.* Upstill-Goddard et al.,
523 1996). Depending upon the volume of sample analyzed, purge-and-trap analysis can have a
524 detection limit much lower than 1 nmol kg^{-1} (*e.g.* Wilson et al., 2017). Methane measurements
525 in aquatic habitats with methane concentrations near the limit of analytical detection include
526 mesopelagic and high latitude environments distal from coastal or benthic inputs (*e.g.* Rehder et

527 al., 1999; Kitidis et al., 2010; Fenwick et al., 2017). Of additional concern is that the skewed
528 distribution of methane concentrations also occurs in samples collected both from the surface
529 ocean (PAC2; Fig. 1b) and coastal environments (BAL1; Fig. 1c). Methane concentrations
530 between 2–6 nmol kg⁻¹ are within the detection limit of all participating laboratories. To address
531 this we recommend that laboratories restrict sample storage to the minimum time required to
532 analyze the samples and incorporate internal controls into their sample analysis (Section 4.4).

533 There was an improvement in the overall agreement between the laboratories for samples
534 with higher methane concentrations. However, some of the highest variability between the
535 laboratories was observed at the highest concentrations of methane analyzed (BAL2; Fig. 1e).
536 This high degree of variability resulted in significant uncertainty in the absolute *in situ*
537 concentration. Methane concentrations of this magnitude and higher are found in coastal
538 environments (Zhang et al., 2004; Jakobs et al., 2014; Borges et al., 2017) and in the water-
539 column associated with seafloor emissions (*e.g.* Pohlman et al., 2011). These environments are
540 considered vulnerable to climate induced changes and eutrophication, and therefore it is
541 necessary that independent measurements are conducted to the highest possible accuracy to
542 allow for inter-laboratory and inter-habitat comparisons. To address this we recommend that
543 reference material be produced and distributed between laboratories.

544
545 **Nitrous oxide:** Some of the trends discussed for methane were also evident in the nitrous oxide
546 data. For the samples with the lowest nitrous oxide concentrations a skewed data distribution
547 was observed, as found for methane (Fig. 4c). Such low nitrous oxide concentrations are typical
548 of low-oxygen water-column environments (<10 μmol kg⁻¹). Therefore, the analytical bias
549 towards measuring values higher than the absolute *in situ* concentrations is particularly pertinent
550 to oceanographers measuring nitrous oxide in oxygen minimum zones and other low-oxygen
551 environments (Naqvi et al., 2010; Farías et al., 2015; Ji et al., 2015). The low concentrations of
552 nitrous oxide still exceed detection limits by at least an order of magnitude for even the less-
553 sensitive headspace method due to the high sensitivity of the ECD. Therefore, the bias towards
554 reporting elevated values for low concentrations of nitrous oxide is related less to analytical
555 sensitivity and is more a consequence of calibration issues. During the intercomparison exercise
556 ECD calibration was identified as a nontrivial issue for all participating laboratories and it
557 deserves continuing attention. In particular, the nonlinearity of the ECD means that low and

558 high nitrous oxide concentrations are more vulnerable to error since the values fall outside of the
559 most frequented part of the calibration curve. This is particularly true if a linear fit is used to
560 calibrate the ECD (Fig. 6a). To circumvent this problem, one laboratory used a step-wise linear
561 function while other laboratories used a quadratic function. The usefulness of multiple
562 calibration curves for low and high nitrous oxide concentrations was highlighted during the
563 intercomparison exercise, although this necessitates some consideration of the threshold for
564 switching **between** different calibration curves.

565 The majority of seawater samples analyzed had nitrous oxide concentrations ranging from 7–
566 11 nmol kg⁻¹ (Fig. 4a, 4b), which are close to atmospheric equilibrium values, as shown for the
567 Pacific Ocean (Fig. 4b). Collective analysis of these samples gives insight into the precision and
568 accuracy associated with surface water nitrous oxide analysis (Fig 5a). This is discussed further
569 in the context of implementing internal controls for methane and nitrous oxide (Section 4.4). For
570 samples with the highest nitrous oxide concentrations, *i.e.* exceeding 30 nmol kg⁻¹, there was
571 high variability between the concentrations reported by the independent laboratories. This was
572 most evident for the BAL5 samples (Fig. 4e) and similar to the variability observed at the highest
573 methane concentrations analyzed (Fig. 1e). It is difficult to assess how much of this variability
574 was specifically due to the differences in calibration practices between the laboratories and the
575 differences in gas standards with high nitrous oxide mole fractions, but at least some of it can be
576 attributed to this. These results form the basis for a proposed production of reference material
577 for both trace gases.

578

579 **4.3 Are there general recommendations to reduce uncertainty in the accuracy and** 580 **precision of methane and nitrous oxide measurements?**

581 **There are several analytical recommendations resulting from this study. The use of highly**
582 **accurate standards and the appropriate calibration fit is an essential requirement for both**
583 **headspace equilibration and the purge-and-trap technique. It was shown that both analytical**
584 **approaches can yield comparable values for methane and nitrous oxide, with the main**
585 **differences observed at low methane concentrations. At sub-nanomolar methane concentrations,**
586 **four out of the six laboratories that reported methane concentrations <1 nmol kg⁻¹ used a purge-**
587 **and-trap analysis.**

588 This study also revealed that sample storage time can be an important factor. Specifically,
589 the results from this study corroborate the findings of Magen et al. (2014) who showed that
590 samples with low concentrations of methane and more susceptible to increased values as a result
591 of contamination. The contamination was most likely due to the release of methane and other
592 hydrocarbons from the septa (Niemann et al., 2015). Since the release of hydrocarbons occurs
593 over a period of time, it is recommended to keep storage time to a minimum and to store samples
594 in the dark. It should be noted that sample integrity can also be compromised due to other
595 factors including inadequate preservation, outgassing, and adsorption of gases onto septa. For all
596 these reasons, it is recommended to conduct an evaluation of sample storage time for the
597 environment that is being sampled.

598 One useful item that was not included as part of the intercomparison exercise but can help
599 decrease uncertainty in the accuracy and precision of methane and nitrous oxide measurements
600 are internal control measurements. Internal controls represent a self-assessment quality control
601 check to validate the analytical method and quantify the magnitude of uncertainty. Appropriate
602 internal controls for methane and nitrous oxide consist of air-equilibrated seawater samples.
603 Their purpose is to provide checks for methane concentrations ranging from 2–3 nmol kg⁻¹ and
604 for nitrous oxide concentrations from 5–9 nmol kg⁻¹. The air used in the equilibration process
605 could be sourced from the ambient environment if sufficiently stable or from a compressed gas
606 cylinder after cross-checking the concentration with the appropriate gas standard. Air-
607 equilibrated samples provide reassurance that the analytical system is providing values within the
608 correct range. Air-equilibrated samples also indicate the certainty associated with calculating the
609 saturation state of the ocean with respect to atmospheric equilibrium. This is particularly
610 relevant when the seawater being sampled is within a few percent of saturation. Finally, these
611 air-equilibrated samples provide an estimate of analytical accuracy, which is infrequently
612 reported for methane or nitrous oxide. At present, only a few studies report the analysis of air-
613 equilibrated seawater alongside water-column samples (Bullister and Wisegarver, 2008; Capelle
614 et al., 2015; Bourbonnais et al., 2017; Wilson et al., 2017). It is likely that wider implementation
615 would facilitate internal assessment of the analytical system. Since the main equipment required
616 is a water-bath and an overhead stirrer, the production is not cost-prohibitive. A
617 recommendation of this intercomparison exercise is that laboratories routinely use air-
618 equilibrated seawater samples to provide an estimate of analytical accuracy.

619 In addition to the self-assessments provided by the analysis of air-equilibrated seawater, this
620 study revealed the need for reference seawater to help assess the accuracy of high concentration
621 methane and nitrous oxide measurements. Reference seawater in this instance refers to batches
622 of dissolved methane and nitrous oxide samples prepared in the laboratory using an equilibrator
623 set-up, as used for dissolved inorganic carbon (Dickson et al., 2007). In the absence of plans for
624 additional intercomparison exercises, the provision of reference seawater will allow laboratories
625 to continue evaluating their own measurements. **Finally, the lessons learned during the**
626 **intercomparison exercises will be the basis for a forthcoming Good Practice Guide for dissolved**
627 **methane and nitrous oxide.**

628

629 **4.4 What are the implications of interlaboratory differences for determining the spatial and** 630 **temporal variability of methane and nitrous oxide in the oceans?**

631 The key outcome of this study was the identification of differences in methane and nitrous oxide
632 concentrations for the same batch of seawater samples measured by several independent
633 laboratories. Emergent from this is the distinct possibility that any given laboratory will
634 incorrectly report data, thereby increasing uncertainty over the saturation states of both gases.
635 The tendency to over-estimate methane concentrations close to atmospheric equilibrium means
636 that marine emissions of methane to the overlying atmosphere will be also overestimated (Bange
637 et al., 1994; Upstill-Goddard and Barnes, 2016). In contrast, for nitrous oxide there does not
638 appear to be either an under-estimation or over-estimation of concentrations. Consequently, there
639 is generally a lower inherent uncertainty in its surface ocean saturation state, as previously
640 proposed (Law and Ling, 2001; Forster et al., 2009).

641 The inter-laboratory differences highlighted by this study should be viewed in the context of
642 numerous individual efforts to assess temporal and/or spatial trends in methane and nitrous oxide
643 by way of time-series observations (Bange et al., 2010; Farías et al., 2015; Wilson et al., 2017;
644 Fenwick and Tortell, 2018), repeat hydrographic survey lines (de la Paz et al., 2017), and single
645 expeditions. While the value of these in integrating the behaviour of methane and nitrous oxide
646 into the hydrography and biogeochemistry of local-regional ecosystems is beyond question, their
647 value would be enhanced by the rigorous cross-validation of analytical protocols. Without this,
648 perceived small temporal and/or spatial changes in water-column concentrations in any given
649 region are difficult to verify unless the data all originate from a single laboratory. In addition,

650 the value of a global methane and nitrous oxide database (*e.g* Bange et al., 2009) would to some
651 extent be compromised by the uncertainty. Taking due account of the analytical variability
652 between laboratories will clearly be vital to any future assessment of the changing methane and
653 nitrous oxide budgets of the oceans.

654

655 **5. Conclusions**

656 Overall, the intercomparison exercise was invaluable to the growing community of ocean
657 scientists interested in understanding the dynamics of dissolved methane and nitrous oxide in the
658 water-column. The level of agreement between independent measurements of dissolved
659 concentrations was evaluated in the context of several contributing factors, including sample
660 analysis, standards, calibration procedures, and sample storage time. Importantly, the
661 intercomparison represents a concerted effort from the scientists involved to critically assess the
662 quality of their data, and to initiate the steps required for further improvements.

663 Recommendations arising from the intercomparison include routine cross-calibration of working
664 gas standards against primary standards, minimizing sample storage time, incorporating internal
665 controls (air-equilibrated seawater) alongside routine sample analysis, and the future production
666 of reference seawater for methane and nitrous oxide measurements. These efforts will help
667 resolve temporal and spatial variability, which is necessary for constraining methane and nitrous
668 oxide emissions from aquatic ecosystems and for evaluating the processes that govern their
669 production and consumption in the water-column.

670 *Acknowledgements:*

671 **During the final stages of this work, our coauthor John Bullister passed away. The**
672 **intercomparison exercise greatly benefited from John's scientific expertise on dissolved gases.**
673 **He will be greatly missed by the oceanographic community.**

674 The methane and nitrous oxide intercomparison exercise was conducted as a Scientific
675 Committee on Ocean Research (SCOR) Working Group which receives funding from the U.S.
676 National Science Foundation (OCE-1546580). Pacific Ocean seawater samples were collected
677 on HOT cruises which are supported by NSF (including the most recent OCE-1260164 to
678 DMK). Baltic Sea seawater samples were collected during Cruise #142 of the RV *Elisabeth*
679 *Mann Borgese*, with the ship-time provided by the Leibniz Institute for Baltic Sea Research
680 Warnemünde. We thank Ligu Guo for help with sampling during the Baltic Sea cruise. The
681 methane and nitrous oxide gas standards were produced via a Memorandum of Understanding
682 between the University of Hawai'i and NOAA-PMEL. Funding for the gas standards was
683 provided by for the Center for Microbial Oceanography: Research and Education (C-MORE;
684 EF0424599 to DMK), SCOR, the EU FP7 funded Integrated non-CO₂ Greenhouse gas
685 Observation System (InGOS) (Grant Agreement #284274), and NOAA's Climate Program
686 Office, Climate Observations Division. Additional support was provided by the Gordon and
687 Betty Moore Foundation #3794 (DMK), the Simons Collaboration on Ocean Processes and
688 Ecology (SCOPE; #329108 to DMK), and the Global Research Laboratory Program (#
689 2013K1A1A2A02078278 to DMK) through the National Research Foundation of Korea (NRF).
690 AVB is a senior research associate at the FRS-FNRS. AES would like to acknowledge NSF
691 OCE-1437310. MP would like to acknowledge the support of the Spanish Ministry of Economy
692 and Competitiveness (CTM2015-74510-JIN). LF received financial support by FONDAP
693 1511009 and FONDECYT N°1161138. Any use of trade names is for descriptive purposes and
694 does not imply endorsement by the U.S. government

695 **References**

- 696 Anderson, B., Bartlett, K., Frolking, S., Hayhoe, K., Jenkins, J., and Salas, W.: Methane and
697 nitrous oxide emissions from natural sources, Office of Atmospheric Programs, US EPA,
698 EPA 430-R-10-001, Washington DC, 2010.
- 699 Arévalo-Martínez, D. L., Beyer, M., Krumbholz, M., Piller, I., Kock, A., Steinhoff, T.,
700 Körtzinger, A., and Bange, H. W.: A new method for continuous measurements of oceanic
701 and atmospheric N₂O, CO and CO₂: performance of off-axis integrated cavity output
702 spectroscopy (OA-ICOS) coupled to non-dispersive infrared detection (NDIR), *Ocean Sci.*,
703 9, 1071–1087, 2013.
- 704 Atkinson, L. P., and Richards, F. A.: The occurrence and distribution of methane in the marine
705 environment, *Deep-Sea Res.*, 14, 673–684, 1967.
- 706 Bange, H. W., Bartell, U. H., Rapsomanikis, S., and Andreae, M. O.: Methane in the Baltic and
707 North Seas and a reassessment of the marine emissions of methane, *Global Biogeochem.*
708 *Cycles*, 8, 465–480, doi:10.1029/94GB02181, 1994.
- 709 Bange, H. W., Rapsomanikis, S., and Andreae, M. O.: Nitrous oxide cycling in the Arabian Sea,
710 *J. Geophys. Res.: Oceans*, 106, 1053–1065, 2001.
- 711 Bange H.W, Bell, T.G., Cornejo, M., Freing, A., Uher, G., Upstill-Goddard, R.C., and Zhang G.
712 MEMENTO: a proposal to develop a database of marine nitrous oxide and methane
713 measurements. *Env. Chem*, 6, 195–197, 2009.
- 714 Bange, H.W., Bergmann, K., Hansen, H.P., Kock, A., Koppe, R., Malien, F., and Ostrau, C.:
715 Dissolved methane during hypoxic events at the Boknis Eck Time Series Station
716 (Eckernförde Bay, SW Baltic Sea), *Biogeosciences.*, 7, 1279–1284, 2010.
- 717 Borges, A.V., Speeckaert, G., Champenois, W., Scranton, M.I., and Gypens, N.: Productivity and
718 temperature as drivers of seasonal and spatial variations of dissolved methane in the Southern
719 Bight of the North Sea, *Ecosystems*, 1–17, 2017.
- 720 Bourbonnais, A., Letscher, R. T., Bange, H. W., Échevin, V., Larkum, J., Mohn, J., N. Yoshida,
721 N., and Altabet, M. A.: N₂O production and consumption from stable isotopic and
722 concentration data in the Peruvian coastal upwelling system, *Global Biogeochem. Cycles*, 31,
723 678–698, 2017.doi:10.1002/2016GB005567.
- 724 Bullister, J. L., and Wisegarver, D. P.: The shipboard analysis of trace levels of sulfur
725 hexafluoride, chlorofluorocarbon-11 and chlorofluorocarbon-12 in seawater, *Deep-Sea Res.*,
726 55, 1063–1074, 2008.

- 727 Bullister, J. L., and Tanhua, T.: Sampling and measurement of chlorofluorocarbons and sulfur
728 hexafluoride in seawater, IOCCP Report No. 14 ICPO Publication Series No. 134, Version 1,
729 2010.
- 730 Bullister, J. L., Wisegarver, D. P., and Wilson, S. T.: The production of methane and nitrous
731 oxide gas standards for Scientific Committee on Ocean Research (SCOR) Working Group
732 #143, <http://udspace.udel.edu/handle/19716/23288>, 2016.
- 733 Bussmann, I., Matousu, A., Osudar, R. and Mau, S.: Assessment of the radio $^3\text{H-CH}_4$ tracer
734 technique to measure aerobic methane oxidation in the water column, *Limnol. Oceanogr.:*
735 *Methods*, 13,.312–327, 2015.
- 736 Butler, J. H., Elkins, J. W., Thompson, T. M., and Egan, K. B.: Tropospheric and dissolved N_2O
737 of the west Pacific and east Indian Oceans during the El Niño Southern Oscillation Event of
738 1987, *J. Geophys. Res.*, 94, 14,865–14,877, 1989.
- 739 Butler, J. H., and Elkins, J. W.: An automated technique for the measurement of dissolved N_2O
740 in natural waters, *Mar. Chem.*, 34, 47–61, 1991.
- 741 Capelle, D. W., Dacey, J. W., and Tortell, P. D.: An automated, high through-put method for
742 accurate and precise measurements of dissolved nitrous oxide and methane concentrations in
743 natural waters, *Limnol. Oceanogr.: Methods*, 13, 345–355, 2015.
- 744 Ciais, P., Dolman, A.J., Bombelli, A., Duren, R., Pregon, A., Rayner, P.J., Miller, C., Gobron,
745 N., Kinderman, G., Marland, G., and Gruber, N.: Current systematic carbon-cycle
746 observations and the need for implementing a policy-relevant carbon observing system,
747 *Biogeosciences*, 11, 3547–3602, 2014.
- 748 Craig, H. and Gordon, L. I.: Nitrous oxide in the ocean and the marine atmosphere, *Geochim.*
749 *Cosmochim. Acta* 27, 949–955, 1963.
- 750 Cutter, G. A.: Intercalibration in chemical oceanography - getting the right number. *Limnol.*
751 *Oceanogr.: Methods*, 11, 418–424, 2013.
- 752 de la Paz, M., García-Ibáñez, M.I., Steinfeldt, R., Ríos, A.F., and Pérez, F.F.: Ventilation versus
753 biology: What is the controlling mechanism of nitrous oxide distribution in the North
754 Atlantic?, *Global Biogeochem. . Cycles*, 31, 745–760, doi: 10.1002/2016GB005507, 2017.
- 755 Dickson, A. G., Sabine, C. L. and Christian, J. R.: Guide to best practices for ocean CO_2
756 measurements, PICES Special Publication 3, 2007.
- 757 Farías, L., Castro-González, M., Cornejo, M., Charpentier, J., Faúndez, J., Boontanon, N. and
758 Yoshida, N.: Denitrification and nitrous oxide cycling within the upper oxycline of the

759 eastern tropical South Pacific oxygen minimum zone. *Limnol. Oceanogr.*, 54, 132–144,
760 2009.

761 Farías, L., Besoain, V., and García-Loyola, S.: Presence of nitrous oxide hotspots in the coastal
762 upwelling area off central Chile: an analysis of temporal variability based on ten years of a
763 biogeochemical time series, *Environ. Res. Lett.*, 10, 044017, 2015.

764 Fenwick, L., and Tortell, P. D.: Methane and nitrous oxide distributions in coastal and open
765 ocean waters of the Northeast Subarctic Pacific during 2015–2016, *Mar. Chem.*, 200, 45–56,
766 2018.

767 Fenwick, L., Capelle, D., Damm, E., Zimmermann, S., Williams, W. J., Vagle, S., and Tortell, P.
768 D.: Methane and nitrous oxide distributions across the North American Arctic Ocean during
769 summer, 2015, *J. Geophys. Res.: Oceans*, 122, 390–412, doi:10.1002/2016JC012493, 2017.

770 Forster, G., Upstill-Goddard, R. C., Gist, N., Robinson, C., Uher, G. and Woodward, E. M. S.:
771 Nitrous oxide and methane in the Atlantic Ocean between 50 N and 52 S: latitudinal
772 distribution and sea-to-air flux, *Deep-Sea Res.*, 56, 964–976, 2009.

773 Freing, A., Wallace, D. W. R., and Bange, H. W.: Global oceanic production of nitrous oxide,
774 *Phil. Trans. R. Soc. B*, 367, 1245–1255, 2012.

775 Gülzow, W., Rehder, G., Schneider, B., Schneider, J., Deimling, V., and Sadkowiak, B.: A new
776 method for continuous measurement of methane and carbon dioxide in surface waters using
777 off-axis integrated cavity output spectroscopy (ICOS): An example from the Baltic Sea,
778 *Limnol. Oceanogr.: Methods*, 9, 176–184, 2011.

779 Jakobs, G., Holterman, P., Berndmeyer, C., Rehder, G., Blumenberg, M., Jost, G., Nausch, G.,
780 and Schmale, O.: Seasonal and spatial methane dynamics in the water column of the central
781 Baltic Sea (GotlandSea), *Cont. Shelf Res.*, 91, 12–25, 2014.

782 Ji, Q., Babbín, A. R., Jayakumar, A., Oleynik, S., and Ward, B. B.: Nitrous oxide production by
783 nitrification and denitrification in the Eastern Tropical South Pacific oxygen minimum zone,
784 *Geophys. Res. Lett.*, 42, 10,755–10,764, doi:10.1002/2015GL066853, 2015.

785 Kitidis, A., Upstill-Goddard, R. C., and Anderson, L. G.: Methane and nitrous oxide in surface
786 water along the North-West Passage, Arctic Ocean, *Mar. Chem.*, 121, 80–86, 2010.

787 Law, C. S., and Ling, R. D.: Nitrous oxide flux and response to increased iron availability in the
788 Antarctic Circumpolar Current, *Deep-Sea Res.*, 48, 2509–2527, 2001.

789 Magen, C., Lapham, L. L., Pohlman, J. W., Marshall, K., Bosman, S., Casso, M., and Chanton, J.
790 P.: A simple headspace equilibration method for measuring dissolved methane, *Limnol.*
791 *Oceanogr.: Methods*, 12, 637–650, 2014.

- 792 McAuliffe, C.: Solubility on water of C₁-C₉ hydrocarbons, *Nature*, 200, 1092–1093, 1963.
- 793 Myhre, G., Shindell, D., Bréon, F.-M., Collins, W., Fuglestedt, J., Huang, J., Koch, D.,
794 Lamarque, J.-F., Lee, D., Mendoza, B., Nakajima, T., Robock, A., Stephens, G., Takemura,
795 T., and Zhang, H.: Anthropogenic and Natural Radiative Forcing, In: *Climate Change 2013:
796 The Physical Science Basis. Contribution of Working Group I to the Fifth Assessment Report
797 of the Intergovernmental Panel on Climate Change* [Stocker, T. F., Qin, D., Plattner, G.-K.,
798 Tignor, M., Allen, S. K., Boschung, J., Nauels, A., Xia, Y., Bex, V., and Midgley, P. M.
799 (eds.)]. Cambridge University Press, Cambridge, United Kingdom and New York, NY, USA,
800 2013.
- 801 Naqvi, S. W. A., Bange, H. W., Farías, L., Monteiro, P. M. S., Scranton, M. I., and Zhang, J.:
802 Marine hypoxia/anoxia as a source of CH₄ and N₂O, *Biogeosciences*, 7, 215–2190, doi:
803 10.5194/bg-7-2159-2010, 2010.
- 804 National Research Council: *Applications of analytical chemistry to oceanic carbon cycle studies.*
805 Washington DC. National Academy Press, 1993.
- 806 Nevison, C. D., Weiss, R. F., and Erickson, D. J.: Global oceanic emissions of nitrous oxide, *J.*
807 *Geophys. Res.*, 100, 15809–15820, doi: 10.1029/95JC00684, 1995.
- 808 Niemann, H., Steinle, L., Brees, J., Bussmann, I., Treude, T., Krause, S., Elvert, M., and
809 Lehmann, M. F.: Toxic effects of lab-grade butyl rubber stoppers on aerobic methane
810 oxidation, *Limnol. Oceanogr.: Methods*, 13, 40–52, 2015.
- 811 Pohlman, J. W., Bauer, J. E., Waite, W. F., Osburn, C. L., and Chapman, N. R.: Methane
812 hydrate-bearing seeps as a source of aged dissolved organic carbon to the oceans, *Nature*
813 *Geosci.*, 4, 37–41, 2011.
- 814 Reeburgh, W. S.: Oceanic methane biogeochemistry, *Chem. Rev.*, 107, 486–513, doi:
815 10.1021/cr050362v, 2007.
- 816 Rehder, G., Keir, R. S., Suess, E., and Rhein, M.: Methane in the northern Atlantic controlled by
817 microbial oxidation and atmospheric history, *Geophys. Res. Lett.*, 26, 587–590, doi:
818 10.1029/1999GL900049, 1999.
- 819 Schmale, O., Schneider von Deimling, J., Gülzow, W., Nausch, G., Waniek, J. J. and Rehder, G.:
820 Distribution of methane in the water column of the Baltic Sea. *Geophys. Res. Lett.*, 37,
821 L12604, doi: 10.1029/2010GL043115, 2010.
- 822 Strady, E., Pohl, C., Yakushev, E. V., Krügera, S., and Hennings, U.: PUMP–CTD-System for
823 trace metal sampling with a high vertical resolution. A test in the Gotland Basin, Baltic Sea,
824 *Chemosphere*, 70, 1309–1319, 2008.

- 825 Swan, H. B., Armishaw, P., Iavetz, R., Alamgir, M., Davies, S. R., Bell, T. G., and Jones, G. B.:
826 An interlaboratory comparison for the quantification of aqueous dimethylsulfide. *Limnol.*
827 *Oceanogr.: Methods*, 12, 784–794, 2014.
- 828 Upstill-Goddard, R. C., Rees, A. P., and Owens, N. J. P.: Simultaneous high-precision
829 measurements of methane and nitrous oxide in water and seawater by single phase
830 equilibration gas chromatography, *Deep-Sea Res.*, 43, 1669–1682, 1996.
- 831 Upstill-Goddard, R. C., and Barnes, J.: Methane emissions from UK estuaries: Re-evaluating the
832 estuarine source of tropospheric methane from Europe, *Mar. Chem.*, 180, 14–23, 2016.
- 833 Walter, S., Peeken, I., Lochte, K., Webb, A., and Bange, H. W.: Nitrous oxide measurements
834 during EIFEX, the European Iron Fertilization Experiment in the subpolar South Atlantic
835 Ocean, *Geophys. Res. Lett.*, 32, doi:10.1029/2005GL024619, 2005.
- 836 Weiss, R. F., and Price, B. A.: Nitrous oxide solubility in water and seawater, *Mar. Chem.*, 8,
837 347–359, doi: 10.1016/0304-4203(80)90024-9, 1980.
- 838 Weiss, R. F., Van Woy, F. A., and Salameh, P. K.: Surface water and atmospheric carbon
839 dioxide and nitrous oxide observation by shipboard automated gas chromatography: Results
840 from expeditions between 1977 and 1990, Scripps Institution of oceanography Reference 92-
841 11. ORNL/CDIAC-59, NDP-044. Carbon Dioxide Information Analysis Center, Oak Ridge
842 National Laboratory, Tennessee, 1992.
- 843 Wiesenburg, D. A., and Guinasso, N. L.: Equilibrium solubilities of methane, carbon monoxide
844 and hydrogen in water and seawater, *J. Chem. Eng. Data*, 24, 354–360, doi:
845 10.1021/je60083a006, 1979.
- 846 Wilson, S. T., Ferrón, S., and Karl, D. M.: Interannual variability of methane and nitrous oxide in
847 the North Pacific Subtropical Gyre, *Geophys. Res. Lett.*, 44, doi: 10.1002/2017GL074458,
848 2017.
- 849 Zhang, G. L., Zhang, J., Kang, Y. B., and Liu, S. M.: Distributions and fluxes of methane in the
850 East China Sea and the Yellow Sea in spring, *J. Geophys. Res.*, 109, C07011,
851 doi:10.1029/2004JC002268, 2004

852 **Table 1.** List of laboratories that participated in the intercomparison. All laboratories measured
 853 both methane and nitrous oxide except U.S. Geological Survey (methane only), U.C. Santa
 854 Barbara (nitrous oxide only), and NOAA PMEL (nitrous oxide from the Pacific Ocean). Also
 855 indicated are the twelve laboratories that received the SCOR gas standards of methane and
 856 nitrous oxide.

Institution	Lead Scientist	SCOR Standards
University of Hawai'i, USA	Samuel Wilson	Yes
GEOMAR, Germany	Hermann Bange	Yes
Newcastle University, UK	Robert Upstill-Goddard	Yes
Université de Liège, Belgium	Alberto Vieira Borges	No
Plymouth Marine Laboratory, UK	Andrew Rees	Yes
NOAA PMEL, USA	John Bullister	Yes
IIM-CSIC, Spain	Mercedes de la Paz	Yes
CACYTMAR, Spain	Macarena Burgos	No
University of Concepción, Chile	Laura Farías	Yes
IOW, Germany	Gregor Rehder	Yes
University of California Santa Barbara, USA	Alyson Santoro	Yes
National Institute of Water and Atmospheric Research, NZ	Cliff Law	Yes
University British Columbia, Canada	Philippe Tortell	Yes
U.S. Geological Survey, USA	John Pohlman	No
Ocean University of China, China	Guiling Zhang	Yes

857

858

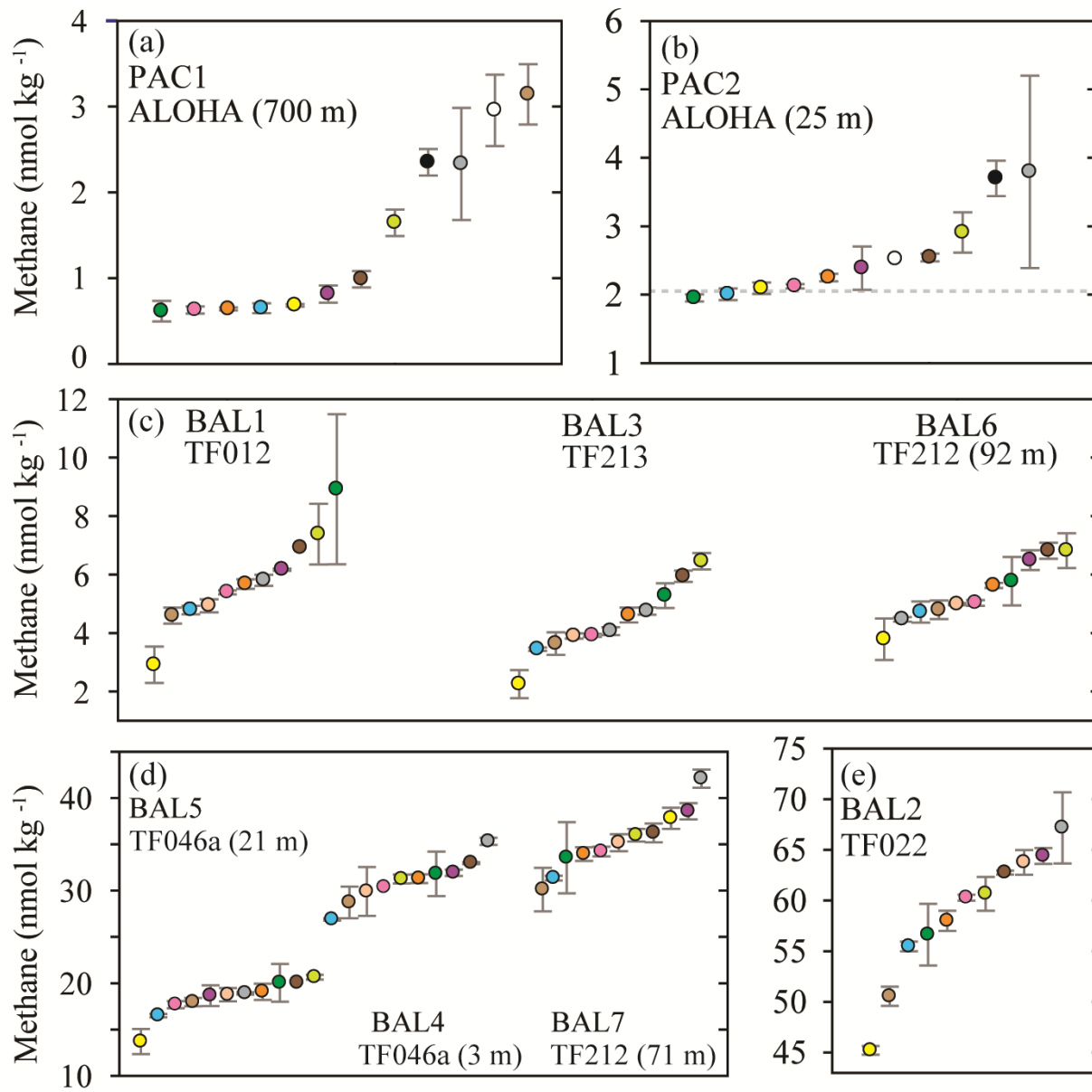
859 **Table 2.** Pertinent information for each batch of methane and nitrous oxide samples. This
 860 includes contextual hydrographic information, median and mean concentrations of methane and
 861 nitrous oxide, range, number of outliers, and the overall average coefficient of variation (%).
 862

Sampling parameters									
Sample ID	PAC1	PAC 2	BAL1	BAL2	BAL3	BAL4	BAL5	BAL6	BAL7
Location	22.75N 158.00W	22.75N 158.00W	54.32N 11.55E	54.11N 11.18E	55.25N 15.98E	55.30N 15.80E	55.30N 15.80E	54.47N 12.21E	54.47N 12.21E
Location name	Station ALOHA	Station ALOHA	TF012	TF022	TF213	TF212	TF212	TF046a	TF046a
Sampling date	24.2.17	24.2.17	16.10.16	17.10.16	18.10.16	19.10.16	20.10.16	21.10.16	21.10.16
Sampling depth (m)	25	700	3	22	3	92	71	3	21
Seawater temperature (°C)	23.6	5.1	12.0	13.6	12.2	6.6	6.7	11.8	13.4
Salinity	34.97	34.23	13.85	17.37	7.87	18.40	18.08	8.81	17.65
Density (kg m ⁻³)	1024	1027	1010	1013	1006	1014	1014	1006	1013
Nitrous oxide									
Number of datasets	13	13	12	13	12	13	12	13	12
Outliers	0	1	2	1	1	0	1	2	2
Median N ₂ O conc. (nmol kg ⁻¹)	42.4	7.0	11.0	9.4	11.1	3.4	40.2	11.0	9.6
Mean N ₂ O conc. (nmol kg ⁻¹)	41.3	7.0	11.1	9.2	11.0	3.4	39.0	10.8	9.5
Range	34.3-45.8	5.9-7.6	10.1-12.7	7.7-11.0	9.6-11.6	2.1-5.5	30.1-45.9	9.5-11.5	8.0-10.4
Average coeff. variation (%)	2.8	4.4	4.5	4.2	2.7	7.5	4.0	2.6	4.4
Methane									
Number of datasets	12	12	11	11	11	11	11	11	11
Outliers	0	1	0	0	0	1	1	0	0
Median CH ₄ conc. (nmol kg ⁻¹)	0.9	2.3	5.7	60.3	4.1	31.3	18.8	5.0	35.2
Mean CH ₄ conc. (nmol kg ⁻¹)	1.8	2.6	5.8	58.6	4.4	31.1	18.8	5.4	35.4
Range	0.6-3.1	1.9-3.8	2.9-8.9	45.2-67.2	2.5-6.5	26.9-35.3	16.5-20.7	3.8-6.8	30.1-42.1
Average coeff. variation (%)	10.9	7.2	8.6	2.1	4.3	3.5	4.2	6.5	3.5

863

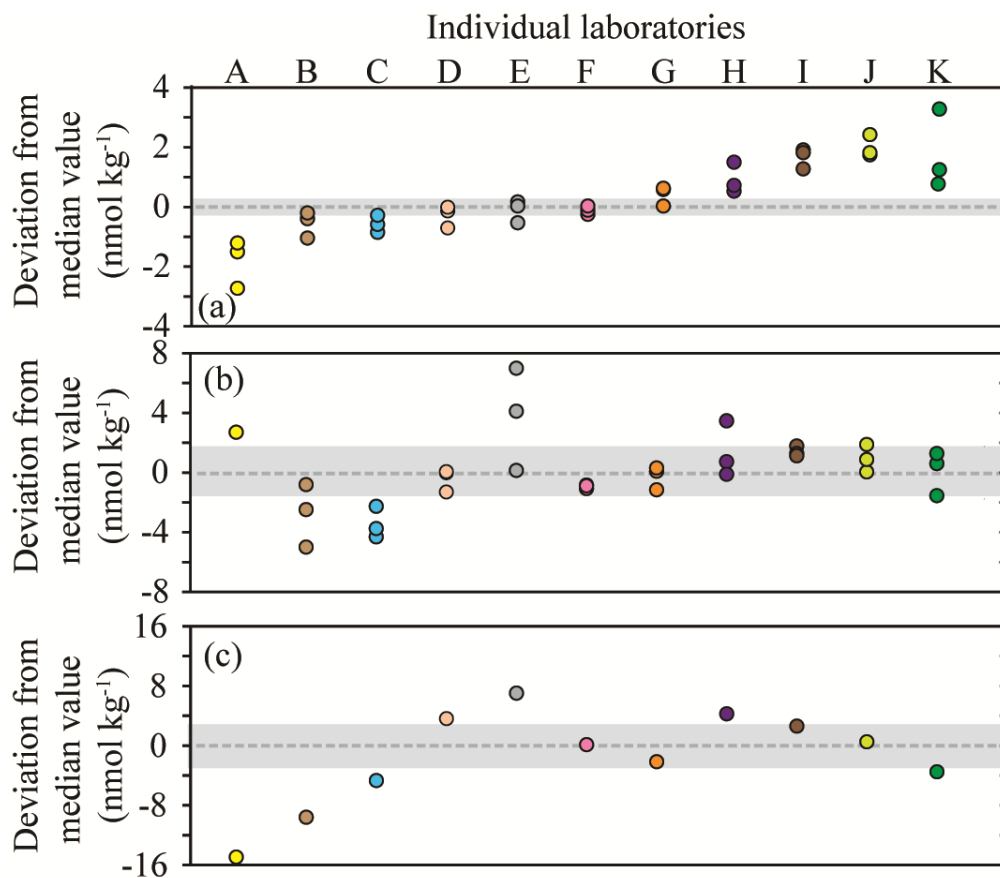
864

865 **Figures**



866
 867
 868 Figure 1. Concentrations of methane measured in nine separate seawater samples collected from
 869 the Pacific Ocean (Fig. 1a, 1b) and the Baltic Sea (Fig. 1c, 1d, 1e). The dashed grey line
 870 represents the value of methane at atmospheric equilibrium (Fig. 1b.) Individual data points are
 871 plotted sequentially by increasing value. The same color symbol is used for each laboratory in
 872 all plots.

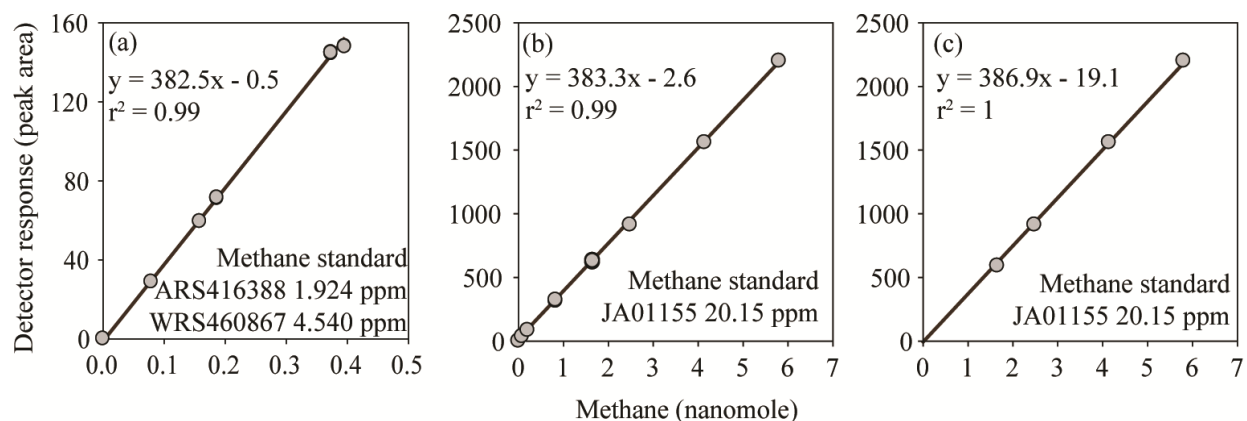
873
 874



875
 876 Figure 2. Deviation from the median methane concentration (reported as absolute values in nmol
 877 kg^{-1}) for the seven Baltic Sea samples. The batches of seawater samples include BAL1, BAL3,
 878 and BAL6 (Fig. 2a), BAL4, BAL5, and BAL7 (Fig. 2b), and BAL2 (Fig. 2c). The shaded grey
 879 area indicates values $\leq 5\%$ of the median concentration. The color scheme for each laboratory
 880 dataset is identical to that used in Figure 1 and the letters allocated to each dataset are to facilitate
 881 cross-referencing in the text. Note that the y-axis scale varies between the Figures.

882

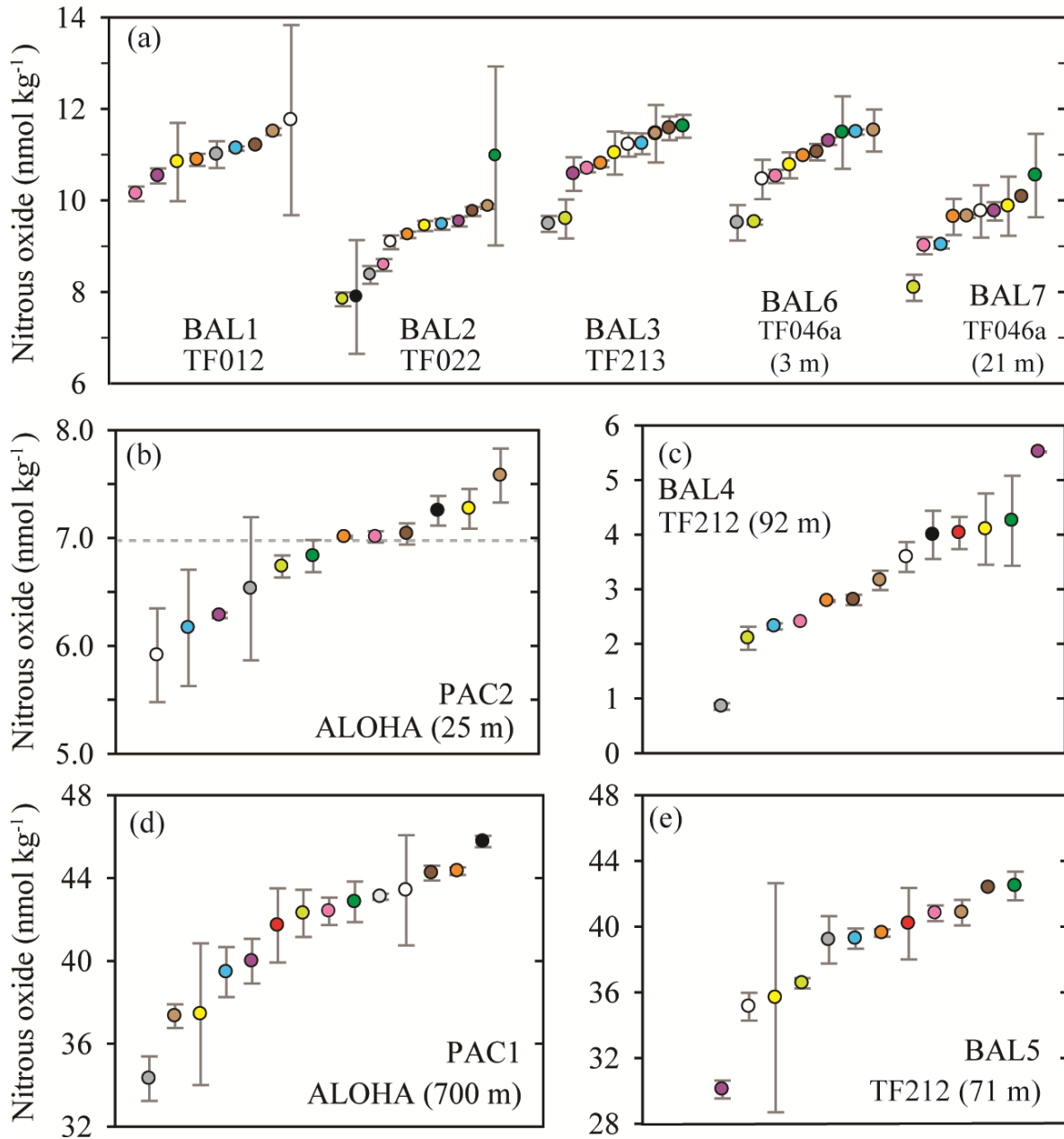
883



884

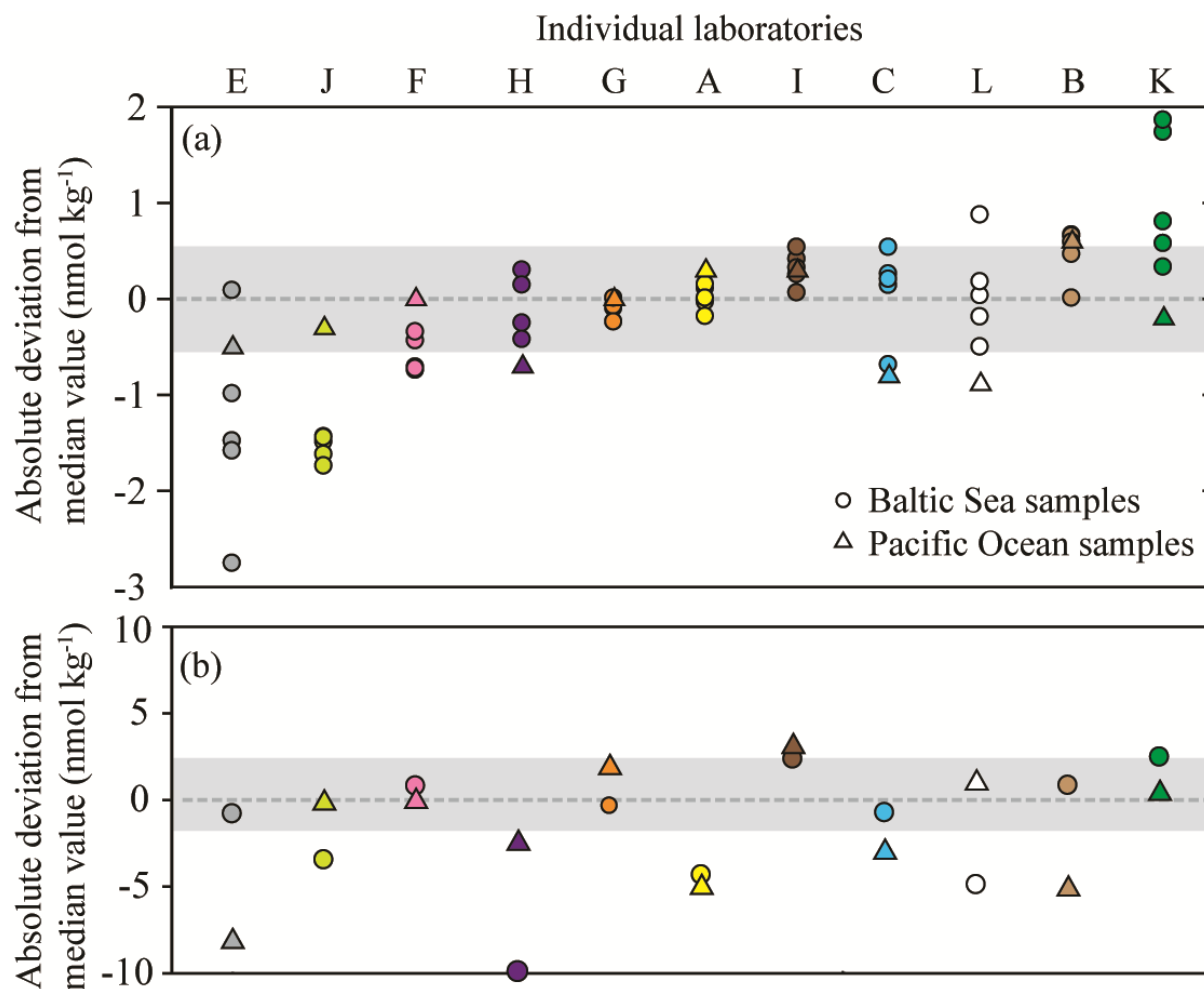
885 Figure 3. FID response to methane, fitted with a linear regression calibration. The inclusion
886 (Fig. 3a and Fig. 3b) or exclusion (Fig. 3c) of low methane values cause the calibration slope and
887 intercept to vary. However, the observed variation in the calibration slope does not have a
888 significant effect on the final calculated concentrations of methane. In contrast, variation in the
889 intercept does have an effect on the final concentrations of methane.

890



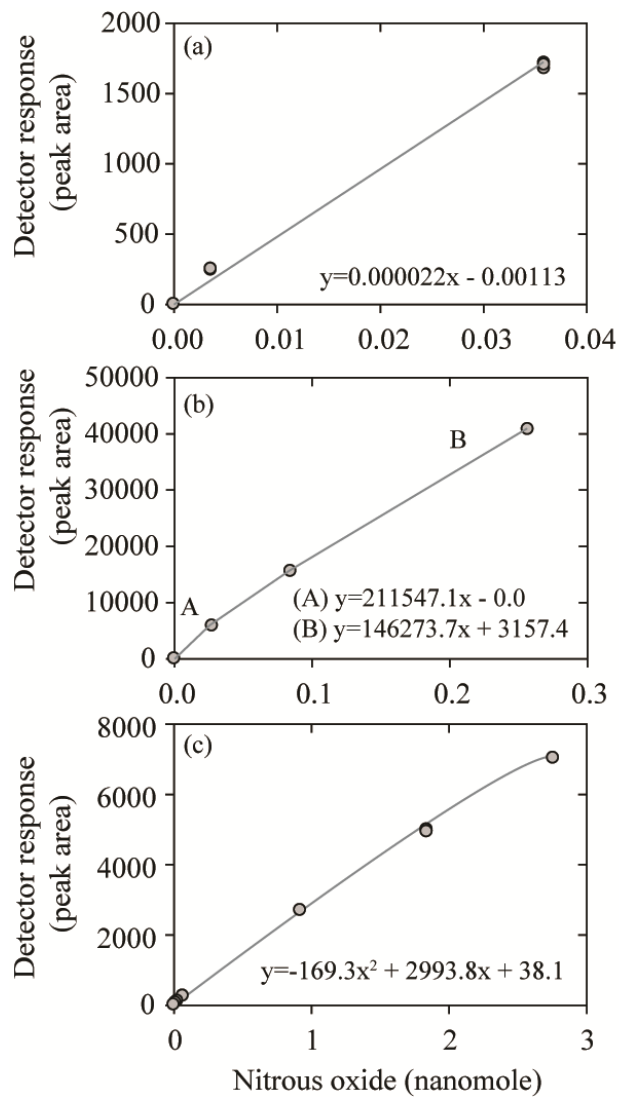
891
 892
 893
 894
 895
 896
 897

Figure 4. Concentrations of nitrous oxide measured in nine separate samples from the Baltic Sea and the Pacific Ocean. The dashed grey line represents the value of nitrous oxide at atmospheric equilibrium (Fig. 4b). Individual data points are plotted sequentially by increasing value. The same color symbol is used for each laboratory in all plots.



898
899

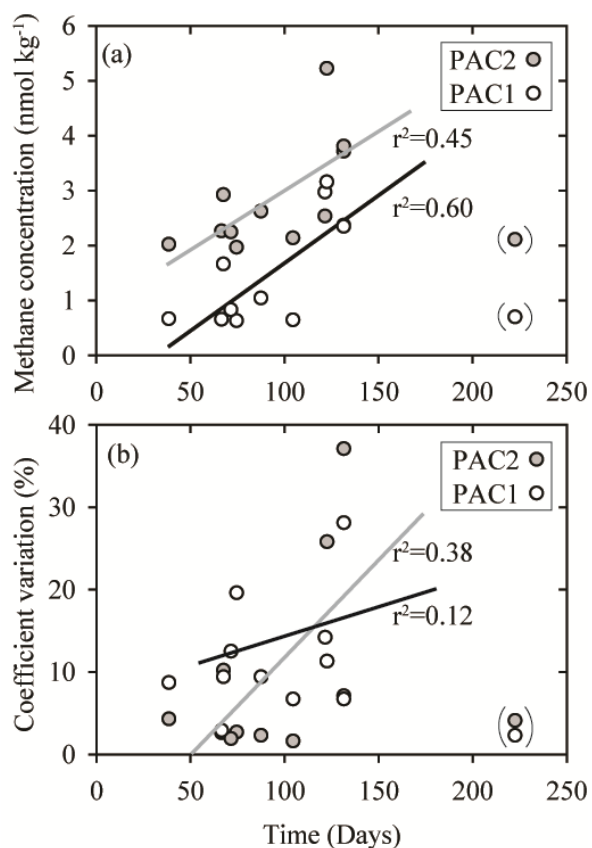
900 Figure 5. Deviation from the median value (reported in absolute units) for nitrous oxide datasets.
 901 The batches of samples include BAL1,2,3,6,7 (Fig. 5a) and PAC2 and BAL5 (Fig. 5b). The
 902 Baltic Sea samples are represented by circles and the Pacific Ocean samples are represented by
 903 triangles. The shaded area indicates a deviation $\leq 5\%$ from the median value, based on a water-
 904 column concentration of 11 nmol kg^{-1} and 42 nmol kg^{-1} for Fig. 5a and 5b, respectively. The
 905 color scheme for each laboratory dataset is identical to that used in Figure 4 and the letters
 906 allocated to each dataset are to facilitate cross-referencing in the text. Note the y-axis for Fig 5a
 907 and 5b are plotted on a different scale.



908

909 Figure 6. Three calibration curves for nitrous oxide measurements using an ECD including linear
 910 (Fig. 6a), multilinear (Fig. 6b), and quadratic (Fig. 6c) fits.

911



912

913 Figure 7. Comparison of sample storage times with measured concentrations of methane (Fig.
914 7a) and coefficient variation (Fig. 7b) for two sets of seawater samples (PAC1 and PAC2)
915 collected in February 2017. These two sets of seawater samples had the lowest methane
916 concentrations and appear to be influenced by the duration of storage time. The data points
917 enclosed in parentheses were not included in the regression analysis. The PAC1 regression line
918 is black and the PAC2 regression line is grey. All of the storage times are included in the
919 Supplementary Material.